Pictorial Essay

Imaging of mucormycosis during the COVID-19 pandemic: A pictorial review

Utsav Ganguly, M.B.B.S.[(1)]
Shalini Agarwal, M.D., D.N.B. [(1)]
Bhavna Arora, D.N.B.[(1)]
Aditya Bhargava, M.S.[(2)]
Virender Singh, M.D.S.[(3)]
Chandni Sharma, M.S.[(2)]
From [(1)] Department of Radiodiagnosis,
[(2)] Department of ENT,
[(3)] Department of oral and maxillofacial surgery,
Pt B.D. Sharma PGIMS, Rohtak 124001 (Haryana), India.
Address correspondence to U.G. (e-mail: utsav.ganguly22@gmail.com)

Received 25 August 2021 ; revised 25 December 2021 ; accepted 28 January 2022
doi:10.46475/aseanjr.v23i1.150

Abstract

During the second wave of the coronavirus disease 2019 (COVID-19) pandemic, there was a significant rise in cases of rhino-orbito-cerebral mucormycosis (ROCM), an invasive form of acute fungal rhinosinusitis with a propensity for rapid spread to the orbits and intracranial compartment.

Prompt diagnosis and subsequent intervention in the form of surgical debridement and administration of antifungals is the mainstay of management of ROCM. Radiology plays a key role in the diagnosis of the disease and in the assessment of the extent of spread. This article serves to elaborate on the significant

THE ASEAN JOURNAL OF RADIOLOGY
ISSN 2672-9393

computed tomography (CT) and magnetic resonance imaging (MRI) findings in patients with ROCM. It is based on imaging findings of 146 microbiologically/histopathologically proven cases that were presented to our institute for management during the second wave (April-June 2021).

While CT gives excellent details of bony anatomy, particularly of bony rarefaction, it has limitations in terms of assessment of soft tissue spread. MRI provides excellent soft tissue delineation and helps with the assessment of the involvement of orbit, particularly the orbital apex, as well as intracranial extension.

Keywords: Mucormycosis, COVID 19, Radiology.

Introduction and pathogenesis

Mucormycosis is a form of zygomycosis, an invasive and rapidly progressive infection caused by fungi of class Zygomycetes and order Mucorales, the most common species being *Rhizopus oryzae*. The first case reported in the literature was in 1885 by Paultauf [1]. However, the first case of mucormycosis was possibly one described by Friedrich Küchenmeister in 1855 [2]. In 1968, Clark proposed the term "mucormycosis" for diseases caused by species of the order Mucorales [3].

Mucormycosis is characterized by extensive angioinvasion with resultant thrombi in blood vessels leading to local gangrene and eschar formation. This might explain the involvement of perisinus soft tissue without frank bony destruction [4].

Rhino-orbito-cerebral mucormycosis (ROCM)

It originates in the paranasal sinuses following the inspiration of spores. Due to angioinvasion, it quickly spreads to the surrounding areas. Symptoms depend on the extent of spread at the time of presentation.
Honavar et al. [5] proposed a four-stage system to determine the anatomical extent and severity of ROCM. These are:
Stage 1: Disease limited to nasal mucosa
Stage 2: Extension into paranasal sinuses
Stage 3: Involvement of orbit
Stage 4: Involvement of CNS

The significant risk factors include diabetes mellitus especially uncontrolled cases, corticosteroid therapy, organ or bone marrow transplantation, neutropenia, trauma, and burns [4]. Diabetes mellitus is an independent risk factor for both severe COVID-19 as well as mucormycosis [6]. Roden et al. found that 33 percent of their 929 patients with ROCM had a history of diabetes [1].

Role of imaging

Imaging determines the extent of spread and plays a crucial role in establishing a diagnosis. The extent of spread dictates the extent of debridement required.

CT is the first-line investigation as it is cheaper and quicker, especially for a high patient load or sick patients. It gives an excellent delineation of rarefaction and focal dehiscence of bone (Figure 1). Extra-sinus spread to the orbital apex and other structures can also be detected on CT. However, very early, subtle involvement might be missed (Figure 2 and 3). It also gives an idea about the normal anatomical variants of the paranasal sinuses, which is important in case of patients planned for Functional Endoscopic Sinus Surgery (FESS) (Figure 4) [7].

THE ASEAN JOURNAL OF RADIOLOGY
ISSN 2672-9393

Middlebrooks et al. performed multivariate analysis and devised a 7-variable model to assess sensitivity, specificity, and positive and negative predictive values for mucormycosis. The variables included periantral fat, bony dehiscence, orbital involvement, septal ulceration, pterygopalatine fossa, nasolacrimal duct, and lacrimal sac. The number of these sites that were involved dictated the sensitivity and specificity for mucormycosis [8].

MRI, on the other hand, provides excellent delineation of soft tissues, both of the intracranial compartment as well as the extracranial head and neck. It can pick up subtle involvement of crucial areas like the orbital apex and cavernous sinus, which may be missed out on a CT scan. MRI is warranted to take a closer look if CT shows abnormalities.

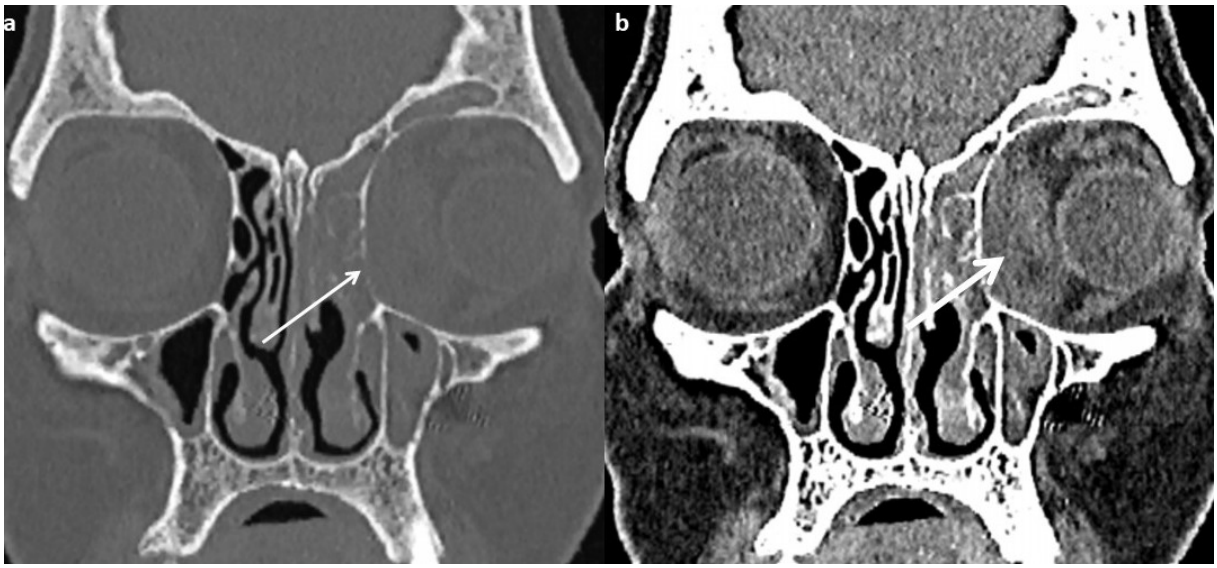

Figure 1. *Coronal reformatted CT in (a) bone and (b) soft tissue window reveals thinning of ethmoid air cells and lamina papyracea (thin arrow). There is a soft tissue lesion in the left ethmoid air cells as well as in the medial aspect of the left orbit with thickening of the medial rectus muscle and displacement of globe laterally (thick arrow).*

Figure 2. *Axial CT shows soft tissue material in the preantral (thin arrow) and the retroantral spaces (thick arrow) on the right side, with bulky muscles of mastication.*

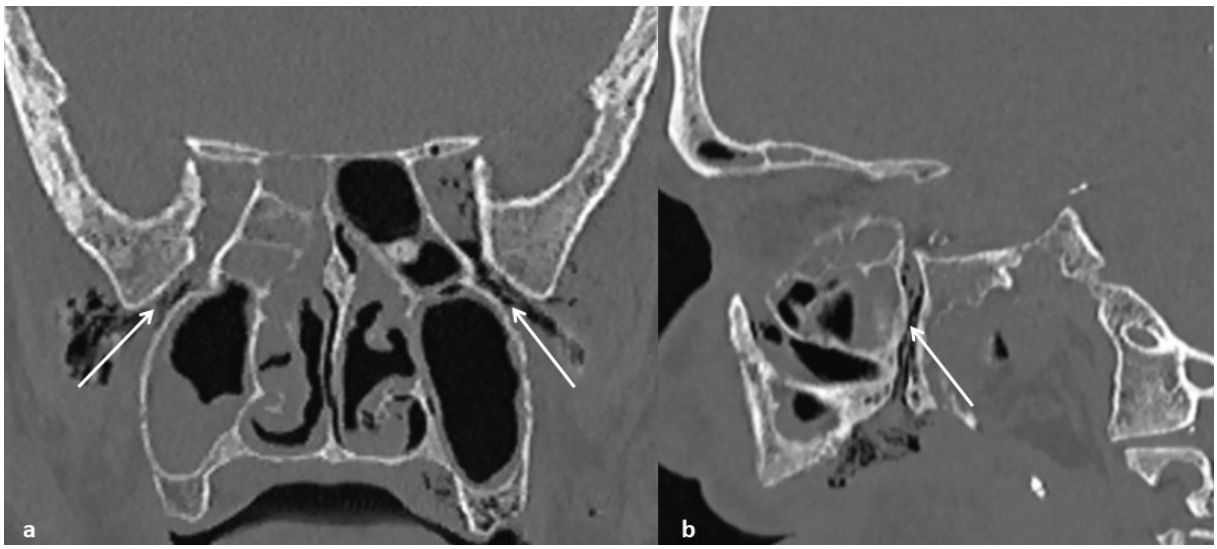

Figure 3. *(a) Coronal reformatted CT shows multiple air foci extending from pterygopalatine fossa to infratemporal fossa bilaterally (arrows). (b) Sagittal reformatted CT shows multiple air foci extending from pterygopalatine fossa to oral cavity via the palatine canal (arrow).*

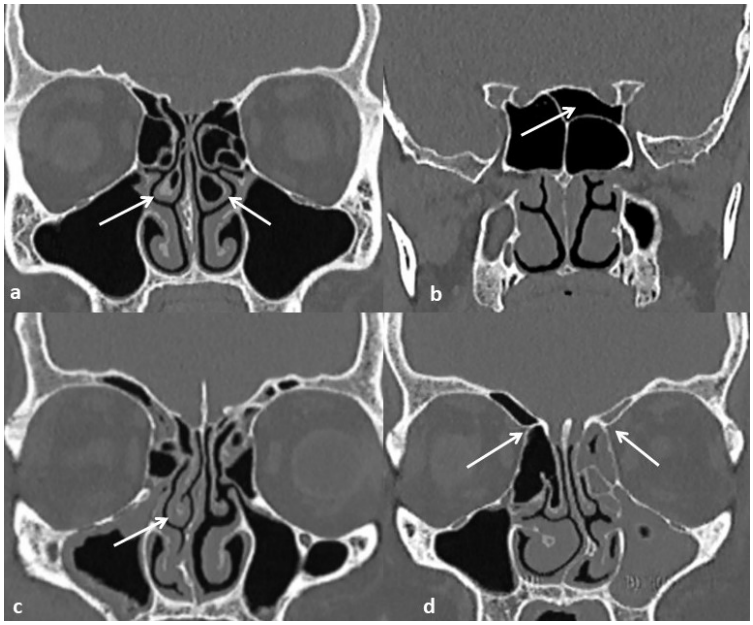

Figure 4. *Coronal reformatted CT showing some common anatomical variants of the paranasal sinuses. (a) Bilateral conchae bullosae (arrows). (b) Onodi cell on the left side (arrow), in close relation to the left optic nerve. (c) Paradoxical curvature of middle turbinate on the right side (arrow). (d) Supraorbital pneumatization, exposing bilateral anterior ethmoid arteries (thin arrows). The ethmoid air cells on the left side are opacified.*

Paranasal sinuses

Non-contrast CT shows soft tissue density material with foci of hyperdensity, which represent calcium phosphate deposits concentrated in areas of mycelium necrosis [9]. (Figure 5). Unilateral soft tissue material in the sinonasal cavity is the most consistent early CT finding, although it is nonspecific [10].

On MRI, the mucosal thickening of sinuses usually appears isointense to grey matter on T1- and hyperintense on T2-weighted images. Sinus contents can show variable signals based on the nature of contents. Fungal elements appear hypointense on T2-weighted sequence due to the presence of heavy metals (Figure 6). Infection can extend into the intracranial compartment via the cribriform plate (Figure 9).

A crucial MRI finding is the black turbinate sign (Figure 7) [11]. Angioinvasive hyphae of mucor cause devitalization of mucosa, which appears as non-enhancing tissue on contrast-enhanced MRI (CE-MRI). It starts in the sinonasal mucosa, particularly the turbinates. On further spread, there is non-enhancement of extraocular muscles of the orbit (Figure 7) and palatal mucosa (Figure 8). However, benign turbinate nonenhancement can be seen in immunocompetent individuals as well, mostly attributed to sinusoids or capacitance vessels that can change size and cause temporary nonenhancement [12].

Figure 5. *Axial CT (a) at the level of the maxillary sinus and (b) at the level of the sphenoid sinus shows hyperdense contents within the left maxillary sinus (thin arrow), sphenoid sinus (black arrow), and left ethmoid air cells (thick arrow). (HU value: 70).*

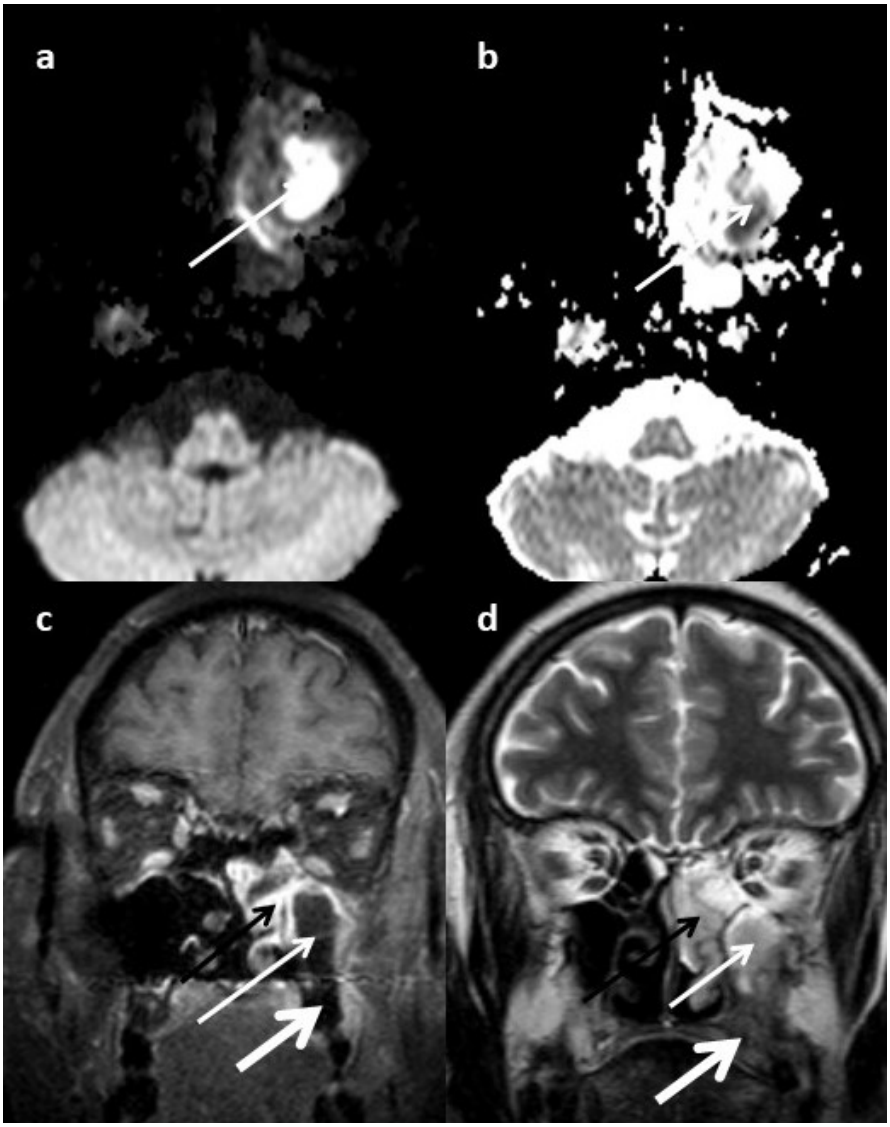

Figure 6. *(a) DWI (b) ADC map (c) Contrast-enhanced coronal image and (d) T2-weighted coronal images at the level of maxillary sinuses show peripherally enhancing mucosal hypertrophy with central non-enhancing contents in the left maxillary sinus (thin arrow). These show diffusion restriction and are seen to extend into the left nasal cavity (black arrow) and the alveolar process inferiorly (thick arrow).*

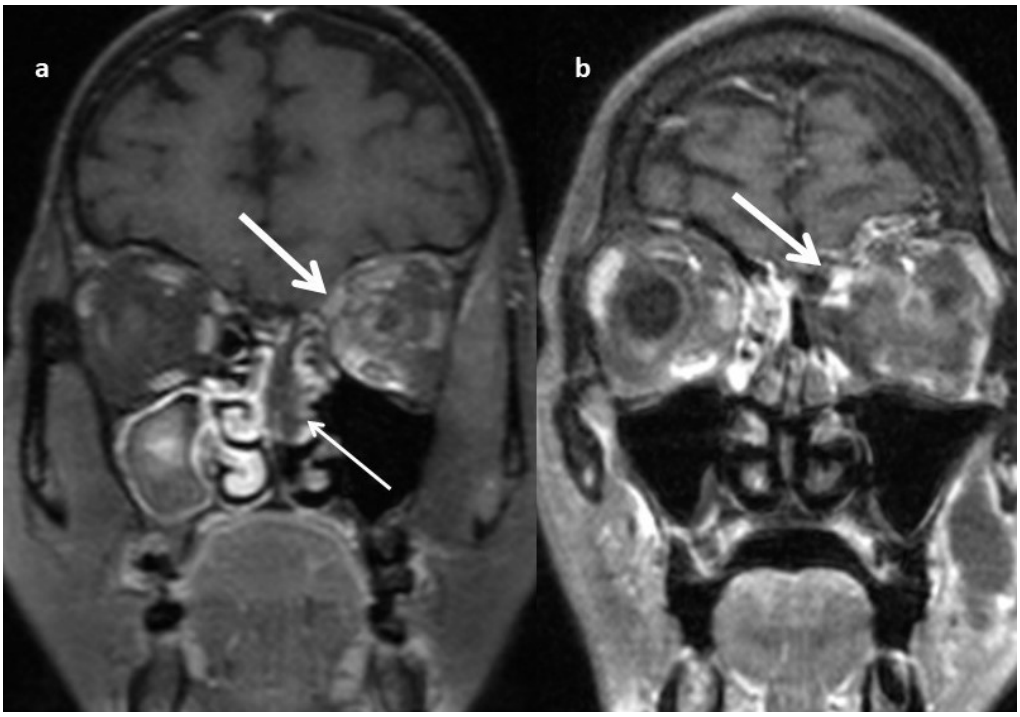

Figure 7. *(a) Coronal contrast-enhanced MRI (CEMRI) shows nonenhancement of middle turbinate on left side (black turbinate sign) (thin arrow). Peripherally enhancing contents with central nonenhancement is seen in the right maxillary sinus. Enhancing inflammatory tissue is seen involving the left superior oblique. (thick arrow). (b) Coronal contrast-enhanced MRI shows non-enhancement of medial rectus and superior oblique (thick arrow) with enhancement in intraconal fat. Non-enhancing tissue is seen involving periantral tissue on left side.*

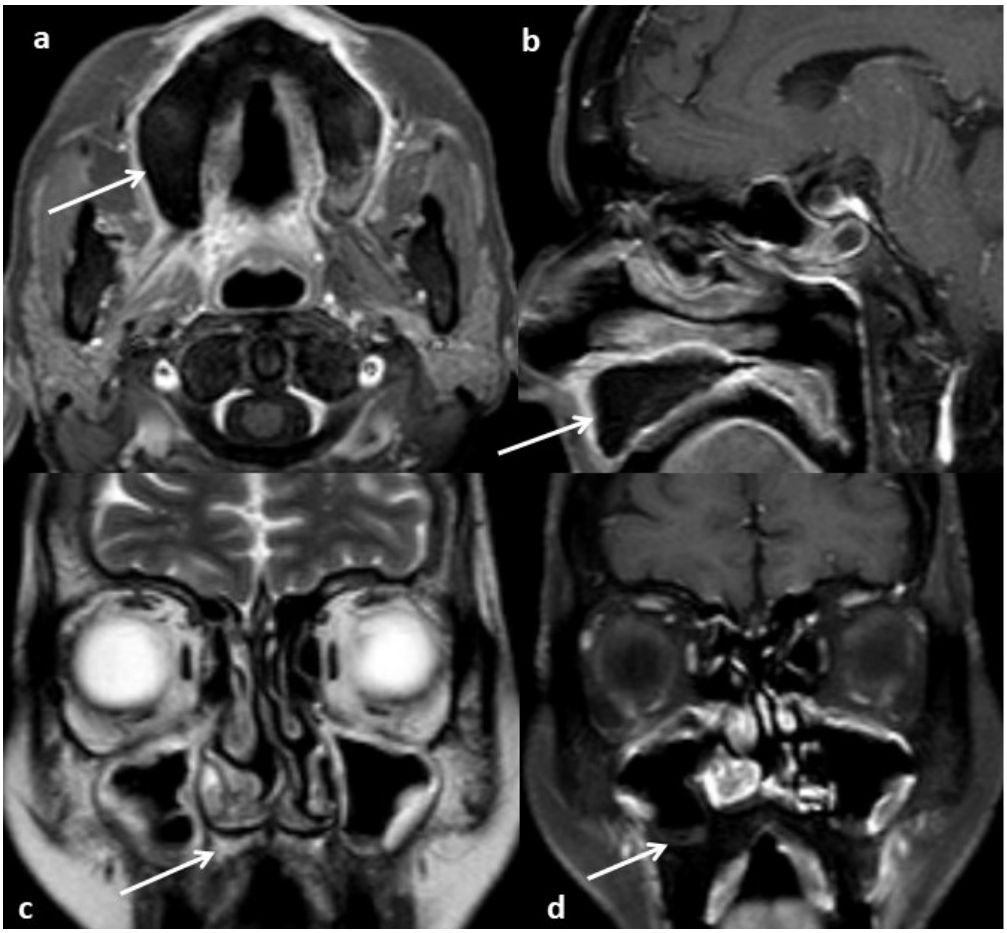

Figure 8. *(a) Axial contrast-enhanced MRI (b) Sagittal contrast-enhanced MRI (c) Coronal T2-weighted MRI and (d) Coronal contrast-enhanced MRI show expansion and nonenhancement of the alveolar process of the maxilla (predominantly on the right side) and the hard palate with peripheral soft tissue enhancement (arrows).*

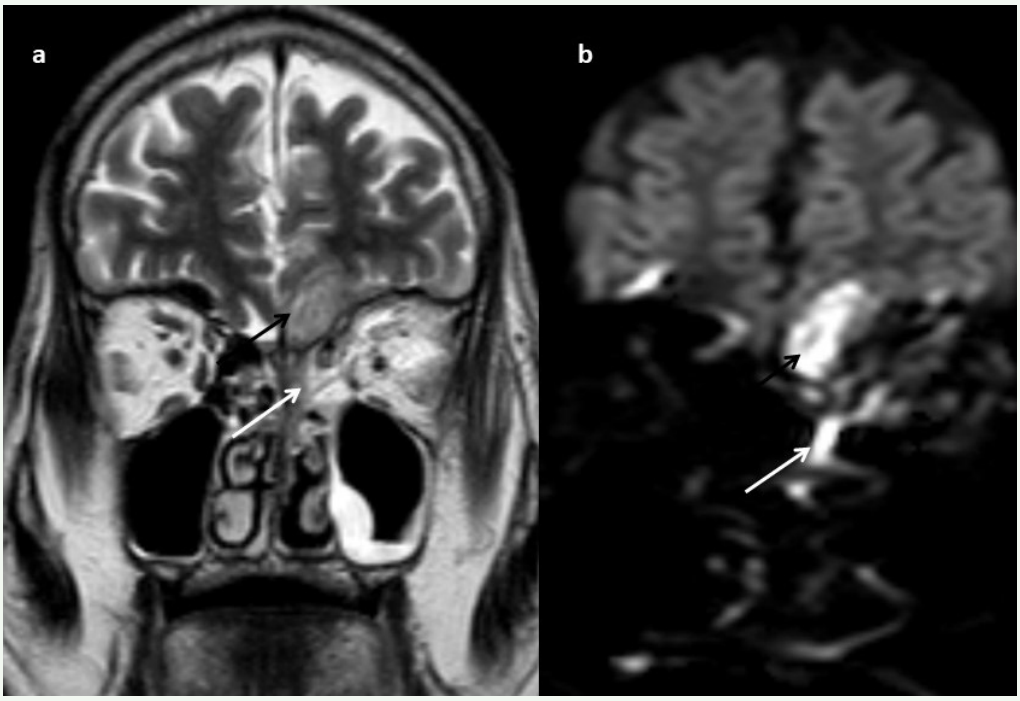

Figure 9. *(a) Coronal T2 weighted MRI and (b) Coronal DWI show extension of infection from ethmoid air cells (white arrows) to the gyrus rectus of the frontal lobe (black arrows), across the cribriform plate. The frontal lobe lesion and the ethmoid contents show intermediate signal intensity on T2-weighted image and restriction on DWI.*

Oral and maxillofacial

Extrasinus spread can involve the neck spaces as well as the maxillofacial area up to the skull base (Figure 2,3,10). MRI is much more sensitive than the soft tissue algorithm of CT to detect extra-sinus spread, characterized by T2/FLAIR hyperintensity, with contrast enhancement interspersed with areas of nonenhancement indicating nonviable tissue [13].

Infection in the maxillary sinus can spread medially into the nasal cavity (Figure 6) and can involve the nasal septum and turbinates. Extension through the other walls involves the extracranial head and neck (Figure 10). Through the anterior wall of the maxillary sinus, the infection spreads to the pre-antral soft tissues (Figure 2). Retro-antral fat can be involved via the posterolateral wall of the maxillary sinus with extension to the infratemporal fossa (Figure 2).

The oral cavity can be involved via the hard palate or the alveolar process of the maxilla (Figure 6), and by perineural spread from the pterygopalatine fossa. (Figure 3). Perineural and perivascular spread occur, mostly along branches of the trigeminal nerve [14], sometimes along the labyrinthine segment of the facial nerve (Figure 3) [15].

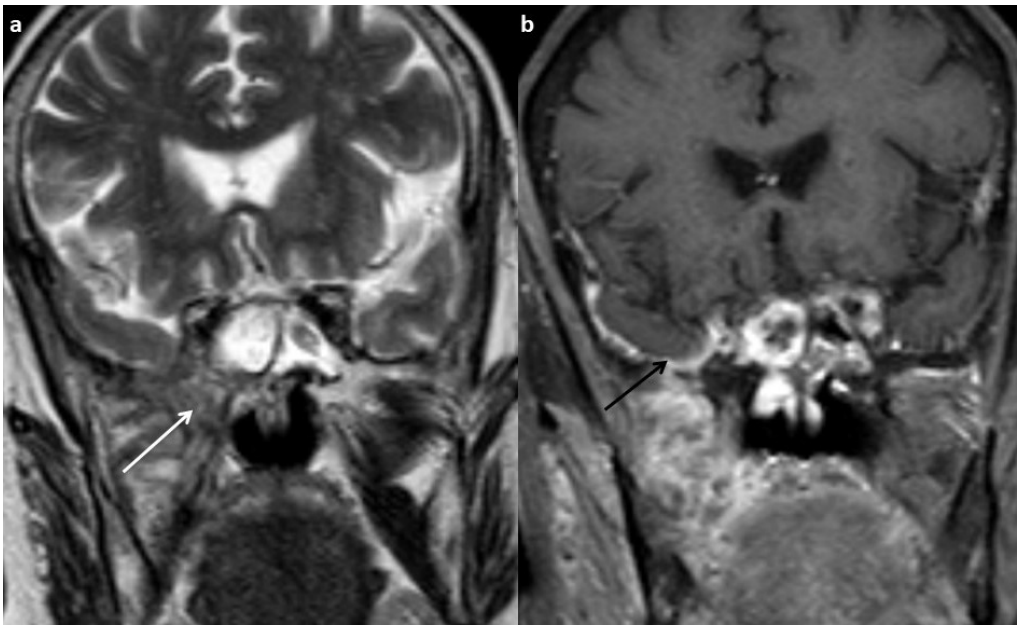

Figure 10. *(a) Coronal T2 weighted MRI and (b) Coronal CEMRI show loss of fat signal in the middle skull base on the right side indicative of skull base involvement (white arrow). The right infratemporal fossa and dura along the right temporal lobe show enhancement (black arrow).*

Orbit

Involvement of the orbit can occur via the maxillary sinus, the pterygopalatine fossa, the lamina papyracea, the or nasolacrimal duct (Figure 1) [13]. NCCT findings include proptosis, thickening and blurring of margins of the optic nerve and extraocular muscles, and orbital fat stranding. Advanced cases can show fullness of the orbital apex (Figure 11).

On contrast studies, the extraocular muscles appear thickened and show a lack of normal contrast enhancement (Figure 7). The optic nerve can appear thickened, show non-enhancement, and sometimes can undergo infarction, showing diffusion restriction (Figure 12) [16]. One of the most dreaded complications of orbital mucormycosis is orbital compartment syndrome (Figure 13).

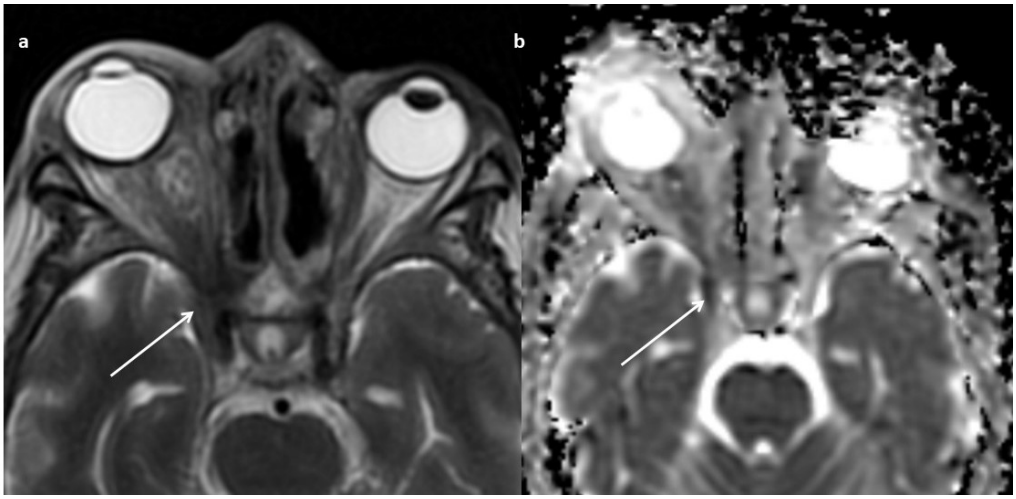

Figure 11. *(a) T2-weighted axial MRI showing involvement of intraconal fat and orbital apex on the right side with extension into cavernous sinus (arrow). (b) ADC map of the same patient shows diffusion restriction in the right cavernous sinus (arrow).*

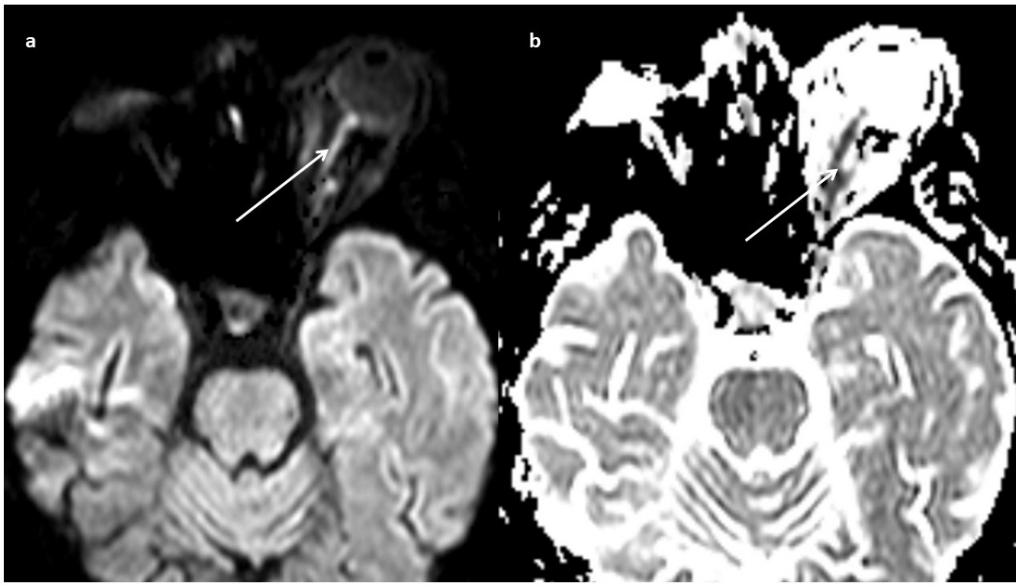

Figure 12. *Axial MRI (a) DWI and (b) ADC map show proptosis of the left globe and restricted diffusion in the left optic nerve (white and black arrow).*

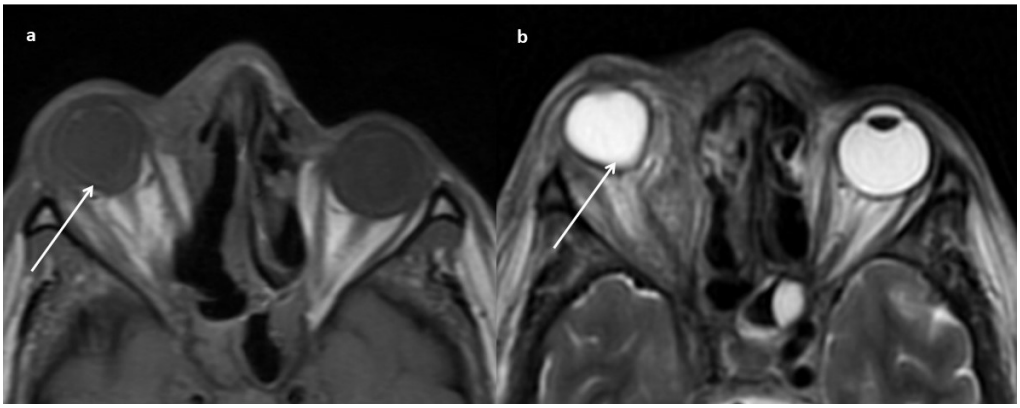

Figure 13. *Axial MRI of the orbit (a) T1-weighted (b) T2-weighted show proptosis, stretching of the optic nerve, and tenting of the globe (guitar pick sign) suggestive of orbital compartment syndrome (white arrows).*

Brain

Intracranial spread occurs via the orbital apex or by direct extension of infection from the sinonasal compartment via the skull base. Osteomyelitis of the skull base manifests as low signal devitalized soft tissue in and around the bony skull base (Figure 10) [15].

Cavernous sinus thrombosis is one of the commonest intracranial manifestations, characterised by loss of flow void of internal carotid artery and nonenhancement on CEMRI (Figure 14).

Direct intracranial invasion can manifest as fungal abscesses. Restricted diffusion is a hallmark of pyogenic brain abscesses; however, findings in fungal abscesses are less specific (Figure 15) [17].

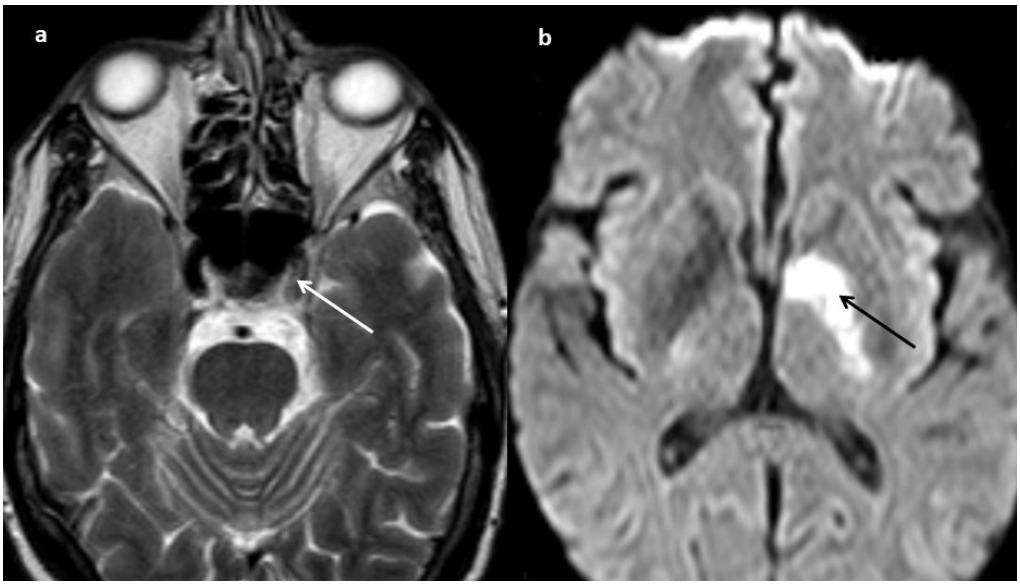

Figure 14. *(a) Axial T2-weighted MRI show loss of flow void of the left internal carotid artery (white arrow). (b) DWI of the same patient shows an acute infarct in the left gangliocapsular region (black arrow).*

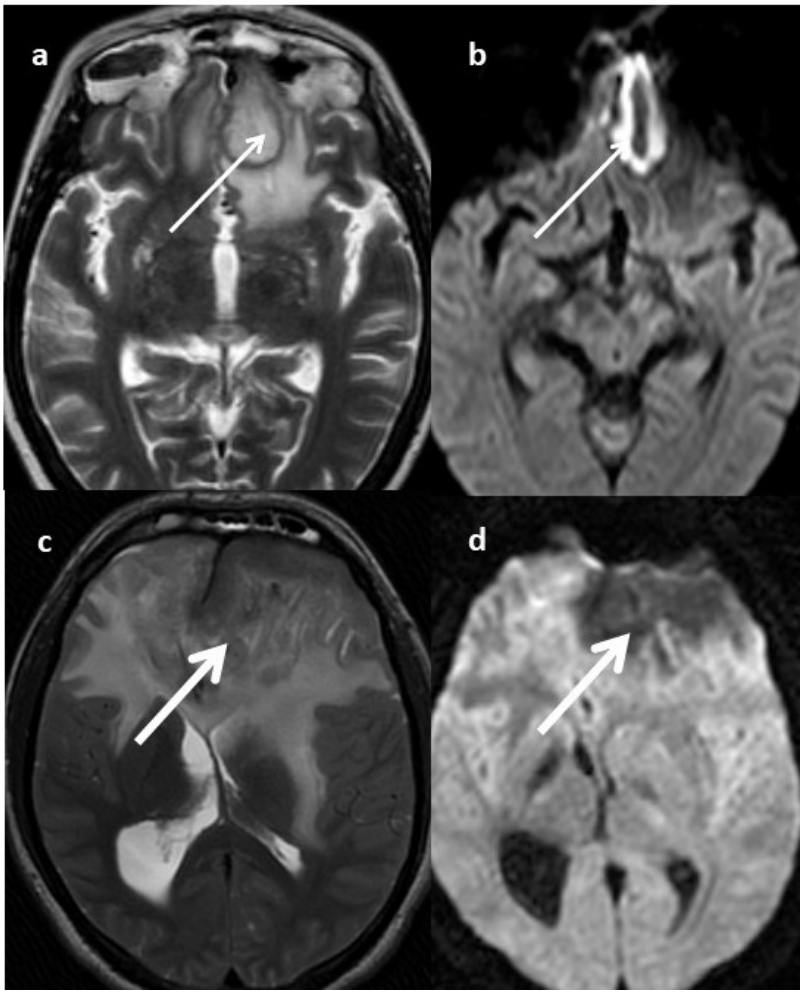

Figure 15. *Axial MRI (a) T2 weighted (b) DWI show a large lesion in the left gyrus rectus with peripheral restriction (thin arrows). Axial MRI (c) T2 weighted (d) DWI in another patient shows a large peripherally enhancing abscess in the left frontal lobe with no diffusion restriction (thick arrows).*

Conclusion

Both CT and MRI play a vital role in the diagnosis and staging of mucormycosis. While CT gives excellent details of bony anatomy, particularly bony rarefaction, it has limitations in terms of assessment of soft tissue spread. MRI remains the mainstay in the assessment of the extent of spread and guide management.

References

1. Roden MM, Zaoutis TE, Buchanan WL, Knudsen TA, Sarkisova TA, Schauflee RL, et al. Epidemiology and outcome of zygomycosis: a review of 929 reported cases. Clin Infect Dis 2005;41:634-53. doi: 10.1086/432579.

2. Chander J. Textbook of medical mycology. 4th ed. New Delhi: Jaypee Brothers Medical Publishers; 2018. p.554-96.

3. Kwon-Chung KJ. Taxonomy of fungi causing mucormycosis and entomophthoramycosis (zygomycosis) and nomenclature of the disease: molecular mycologic perspectives. Clin Infect Dis 2012;54 Suppl 1:S8-15. doi: 10.1093/cid/cir864.

4. Ibrahim AS, Spellberg B, Walsh TJ, Kontoyiannis DP. Pathogenesis of mucormycosis. Clin Infect Dis 2012;54 Suppl 1:S16-22. doi: 10.1093/cid/cir865.

5. Honavar SG. Code Mucor: guidelines for the diagnosis, staging and management of rhino-orbito-cerebral mucormycosis in the setting of COVID-19. Indian J Ophthalmol 2021;69:1361-5. doi: 10.4103/ijo.IJO_1165_21.

6. Singh AK, Singh R, Joshi SR, Misra A. Mucormycosis in COVID-19: a systematic review of cases reported worldwide and in India. Diabetes Metab Syndr 2021;15(4):102146. doi: 10.1016/j.dsx.2021.05.019.

7. O'Brien WT Sr, Hamelin S, Weitzel EK. The preoperative sinus CT: avoiding a "CLOSE" call with surgical complications. Radiology 2016;281:10-21. doi: 10.1148/radiol.2016152230.

8. Middlebrooks EH, Frost CJ, De Jesus RO, Massini TC, Schmalfuss IM, Mancuso AA. Acute invasive fungal rhinosinusitis: a comprehensive update of CT findings and design of an effective diagnostic imaging model. AJNR Am J Neuroradiol 2015 ;36:1529-35. doi: 10.3174/ajnr.A4298.

THE ASEAN JOURNAL OF RADIOLOGY
ISSN 2672-9393

9. Singh V. Fungal rhinosinisitis: unravelling the disease spectrum. J Maxillofac Oral Surg 2019;18:164-79. doi: 10.1007/s12663-018-01182-w.

10. Aribandi M, McCoy VA, Bazan C 3rd. Imaging features of invasive and noninvasive fungal sinusitis: a review. Radiographics 2007;27:1283-96. doi: 10.1148/rg.275065189.

11. Safder S, Carpenter JS, Roberts TD, Bailey N. The "Black Turbinate" sign: an early MR imaging finding of nasal mucormycosis. AJNR Am J Neuroradiol 2010;31:771-4. doi: 10.3174/ajnr.A1808.

12. Han Q, Escott EJ. The black turbinate sign, a potential diagnostic pitfall: evaluation of the normal enhancement patterns of the nasal turbinates. AJNR Am J Neuroradiol 2019;40:855-61. doi: 10.3174/ajnr.A6037.

13. Herrera DA, Dublin AB, Ormsby EL, Aminpour S, Howell LP. Imaging findings of rhinocerebral mucormycosis. Skull Base 2009;19:117-25. doi: 10.1055/s-0028-1096209.

14. Sravani T, Uppin SG, Uppin MS, Sundaram C. Rhinocerebral mucormycosis: pathology revisited with emphasis on perineural spread. Neurol India 2014;62:383-6. doi: 10.4103/0028-3886.141252.

15. Sanghvi D, Kale H. Imaging of COVID-19-associated craniofacial mucormycosis: a black and white review of the "black fungus". Clin Radiol 2021;76:812-9. doi: 10.1016/j.crad.2021.07.004.

16. Hatipoglu HG, Gurbuz MO, Yuksel E. Restricted diffusion in the optic nerve and retina demonstrated by MRI in rhino-orbital mucormycosis. J Neuroophthalmol 2009 ;29:13-5. doi: 10.1097/WNO.0b013e318183bde4.

17. Gaviani P, Schwartz RB, Hedley-Whyte ET, Ligon KL, Robicsek A, Schaefer P, et al. Diffusion-weighted imaging of fungal cerebral infection. AJNR Am J Neuroradiol 2005 ;26:1115-21.